

GEOMETRICAL FIELD ENHANCEMENT ON MICROPATTERNED NANODIAMOND FILM FOR ELECTRON EMISSIONS

K. Subramanian, W. P. Kang, J. L. Davidson, W. H. Hofmeister, B. K. Choi, and M. Howell

Department of Electrical Engineering and Computer Science, Vanderbilt University, TN 37235, USA

Keywords: nanodiamond, chemical vapor deposition, geometrical field enhancement, electron field emission.

Abstract

Introduction: Chemical vapor deposited (CVD) diamond has unique material properties suitable for electron emission such as low electron affinity, hardness to withstand ion bombardment, and good thermal and electrical conductivity to handle high current. In particular, nanocrystalline diamond, apart from excellent chemical, mechanical and thermal characteristics, possesses properties distinct from the conventional CVD microcrystalline diamond including smaller grain size (1 nm-100 nm), higher volume density of grain boundaries, more sp^2 -bonded carbon content, uniform surface morphology, and a wider latitude for materials integration ^[1]. In this paper, we report a robust and reliable technique to micropattern nanodiamond films using reactive ion etching (RIE) process and thereby study the effect of the geometrical field enhancement for electron emissions.

Nanodiamond for field emission: “Cauliflower-like” nanodiamond films with grain size as small as 5-10 nm have been achieved by employing an effective growth-rate control technique through the process of $CH_4/H_2/N_2$ microwave plasma enhanced chemical vapor deposition (MPECVD). We observe that a means to grow nanodiamond films is to increase the nucleation rate and decrease the growth rate by adjusting the CVD process parameters, viz., microwave power, reactant pressure and gas flow rate ^[1]. Raman spectroscopic analysis of the nanodiamond film indicates that the degree of sp^2 -bonded carbon content in the diamond film increases as the grain size decreases. The sp^2/sp^3 peak ratio of the 5-10 nm grain-sized nanodiamond film is found to be ~0.97. The favorable properties of the nanodiamond film, namely, 5 nm grain size, smoother surface morphology, and increased sp^2 -carbon content can be utilized in the development of enhanced field emission devices.

Micropatterned nanodiamond emitter with enhanced field emission geometry: The single-mask fabrication process begins with the growth of a 2- μm thick nanodiamond film on a silicon-on-insulator (SOI) wafer by $CH_4/H_2/N_2$ MPECVD. Next, a 0.5 μm -thick layer of aluminum is deposited on the nanodiamond film to form the masking layer. Conventional photolithography is performed to pattern the emitter structures on the aluminum. The exposed Aluminum is etched away by wet chemical etching and the photoresist removed. With aluminum as mask, the exposed nanodiamond is etched with high selectivity by reactive ion etching (RIE) in pure oxygen plasma. The patterned diamond emitters on the silicon layer are then used as a mask for silicon etching to yield the isolation between the emitters. The final structure consists of patterned nanodiamond emitters, supported by a silicon layer underneath, sitting on the SiO_2 layer on the silicon substrate. Figure 1 displays the SEM micrographs of the micropatterned nanodiamond 6-finger, 4-finger, and edge emitters. The aspect ratio of each emitter finger is ~46 and ~52 in specific cases.

Field emission characterization: The as-deposited nanodiamond film and the micropatterned nanodiamond emitter structures were characterized for field emission in a vacuum of $\sim 10^{-6}$ Torr. Electron emission from the as-deposited nanodiamond film surface was measured using a heavily doped silicon sample as the anode and an insulating spacer of 40 μm , which defined the anode-cathode spacing. The micropatterned nanodiamond finger and edge emitters were tested for field emission laterally with an integrated adjacent anode structure. The field emission characteristics of the three different emitters are presented in Figure 2. The highly linear F-N plots clearly confirm that the current is attributed to field emission. The as-deposited nanodiamond film demonstrated a high turn-on field of 18 V/ μm and 3 μA emission current at an electric field of ~ 30 V/ μm . The 6-fingered nanodiamond emitter exhibited a very low turn-on electric field of 1.9 V/ μm and a high emission current of ~ 104 μA at 20 V/ μm , while the edge emitter, with a 6.5 V/ μm turn-on field, showed 4.6 μA emission current at the same electric field of 20 V/ μm . The effect of the geometry of the high aspect-ratio fingers and the edge emitters on field emission from the nanodiamond film was studied. The emission data of the different emitters was correlated to the modified Fowler-Nordheim equation:

$$\ln(I/E_0^2) = \ln(A * K_1 * \beta^2 / \Phi) - (K_2 * \Phi^{1.5} / \beta) (1/E_0) \quad (1)$$

where K_1 and K_2 are constants, I is the emission current, Φ is the work function of the emitting surface (eV), β is the total field enhancement factor, A is the emitting area, and E_0 is the macroscopic applied electric field (V/cm). Furthermore, the total field enhancement factor β can be expressed in terms of the product of each field enhancement factor as $\beta = \beta_g \beta_{sp^2} \beta_n$, where β_g , β_{sp^2} , β_n are the field enhancement factor due to the geometry, sp^2 -carbon content, and nitrogen doping, respectively. The slope of the linear F-N plot $\{\ln(I/E^2) \text{ vs. } 1/E\}$ is given by $-K_2\Phi^{1.5}/\beta$. The observed field emission enhancement of the micropatterned nanodiamond emitters can be explained by an increase in the geometrical enhancement factor. This can be deduced from the observation that the F-N slope decreases significantly for the fingered and edge emitters (see figure 2 (b)). The reduction of the F-N slope should mainly arise from the geometric effect because the as-deposited nanodiamond film and the nanodiamond emitters have the same sp^2 -carbon and nitrogen concentration and thus should have the same Φ , β_{sp^2} , and β_n . Considering that Φ , β_{sp^2} , and β_n are the same for the nanodiamond films and the micropatterned emitters, β_g can be found from the F-N slopes of emission data. It was found that β_g of the 6-fingered nanodiamond emitter is ~ 198 times that of the as-deposited nanodiamond film and ~ 35 times that of the nanodiamond edge emitter. It was also deduced that the β_g of the edge emitter was ~ 6 times that of the as-deposited nanodiamond film. In order to utilize the excellent geometrical field enhancement offered by the fingered emitters for electron emission, nanodiamond lateral diode has been fabricated employing the process schema outlined in this paper, with the high aspect-ratio fingers serving as the cathode, and the edge structure as the anode, isolated by the SiO_2 layer (see figure 1).

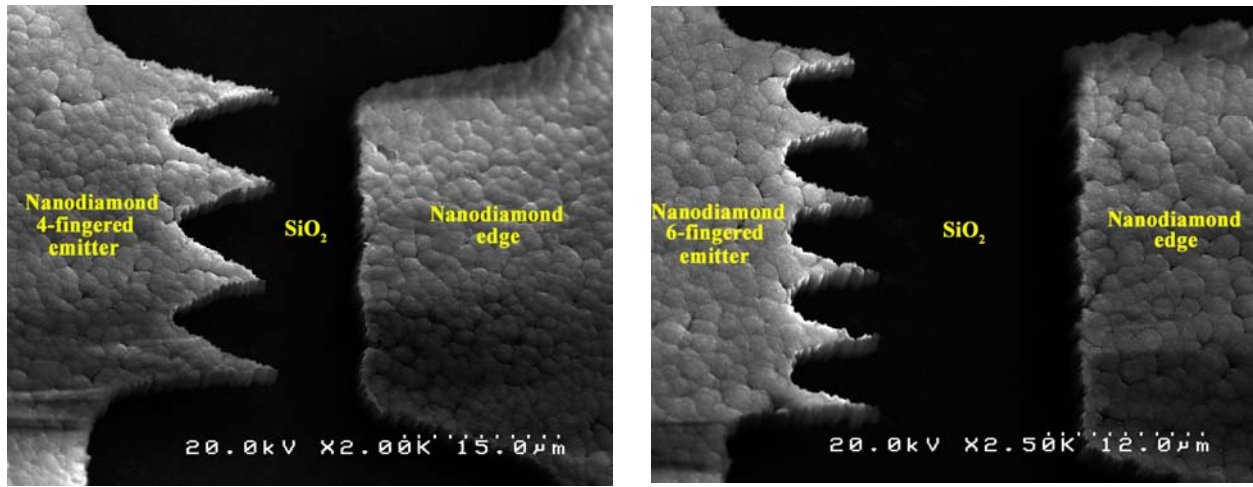


Figure 1. SEM micrographs of the micropatterned nanodiamond lateral field emitters

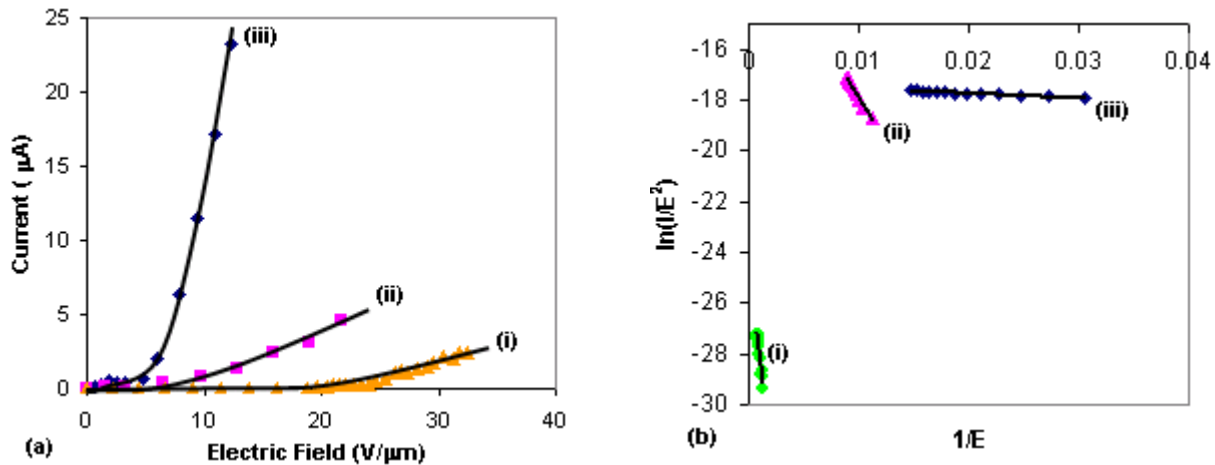


Figure 2. (a) Field emission characteristics of nanodiamond and (b) Corresponding F-N plots: (i) as-deposited nanodiamond film; (ii) nanodiamond edge emitter; (iii) nanodiamond 6-finger lateral emitter

References: [1] K.Subramanian, W.P. Kang, J.L. Davidson, et al., *Proceedings of the 17th IVNC*, pg. 82-83 (2004).

[2] T.D. Corrigan, D.M. Gruen, et al., *Diamond and Related Materials 11*, pp. 43-48, 2002.